NANO LETTERS

2008
Vol. 8, No. 1
69−75

Probing the Structure of DNA–Carbon Nanotube Hybrids with Molecular Dynamics

Robert R. Johnson,[†] A. T. Charlie Johnson,*[,†] and Michael L. Klein[‡]

Department of Physics and Astronomy, Department of Chemistry, University of Pennsylvania, Philadelphia, Pennsylvania 19104

Received August 3, 2007; Revised Manuscript Received November 5, 2007

ABSTRACT

DNA–carbon nanotube hybrids (DNA–CN) are novel nanoscale materials that consist of single-wall carbon nanotubes (SWCN) coated with a self-assembled monolayer of single-stranded DNA (ssDNA). Recent experiments on DNA–CN have shown that this material offers a remarkable set of technologically useful properties such as facilitation of SWCN sorting, chemical sensing, and detection of DNA hybridization. Despite the importance of DNA–CN, a detailed understanding of its microscopic structure and physical properties is lacking. To address this, we have performed classical all-atom molecular dynamics (MD) simulations exploring the self-assembly mechanisms, structure, and energetic properties of this nanomaterial. MD reveals that SWCN induces ssDNA to undergo a spontaneous conformational change that enables the hybrid to self-assemble via the π–π stacking interaction between ssDNA bases and SWCN sidewall. ssDNA is observed to spontaneously wrap about SWCN into compact right- or left-handed helices within a few nanoseconds. Helical wrapping is driven by electrostatic and torsional interactions within the sugar–phosphate backbone that result in ssDNA wrapping from the 3′ end to the 5′ end.

Introduction. Biological molecules can be combined with inorganic nanostructures to form multifunctional hybrid materials with unique properties that will drive advances in nanoelectronics, environmental safety, medicine, and homeland security. One such material of contemporary interest is the DNA−carbon nanotube hybrid (DNA−CN), which consists of a single-wall carbon nanotube (SWCN) coated with a self-assembled monolayer of single-stranded DNA (ssDNA). This unique system offers an intriguing combination of properties derived from an essential, ubiquitous biomolecule and one of the most heralded inorganic nanomaterials.

ssDNA is a complex biological heteropolymer[1] that displays self-recognition in the hybridization of the DNA double helix and can be engineered through "directed evolution" for recognition of other molecular species.[2] SWCNs have a set of unsurpassed physical properties that derive from the completely covalent sp^2 bonding that is characteristic of the defect-free graphene sheet.[3] As examples, SWCN's mechanical stiffness, the carrier mobility of semiconducting SWCNs, and the electrical conductivity of metallic SWCNs are all among the largest of known materials.[3] These two molecular nanostructures are chemically compatible, and are easily combined to form DNA−CN with unique features that arise from the two components. A deeper understanding of this organic/inorganic hybrid nanostructure lies at a powerful advancing frontier of fundamental research in nanoscience and will enable numerous proposed applications of DNA−CN.[4−9]

It was recently shown that SWCN field effect transistors (FETs) decorated with a nanoscale layer of ssDNA display remarkable chemical sensing capabilities with sequence dependent chemical recognition, making them ideal candidates for "electronic nose" applications.[4] Label-free schemes for optical[7] and electronic[8,9] detection of DNA hybridization with DNA−CN have also been reported, and it has been proposed that DNA−CN may provide a means for ultrafast DNA sequencing.[10] Because ssDNA in aqueous solution carries an overall negative charge and contains many polar functional groups, DNA−CNs are water-soluble entities that can be individually suspended in aqueous solution and subsequently sorted according to SWCN electronic properties.[5,6]

The importance of this composite nanomaterial motivates a quantitative understanding of its interactions, structure, and physical properties. Atomic force microscope (AFM) images of DNA−CN based on the poly GT (sequences of repeating guanine and thymine nucleotides) sequence and formed using sonication are reported to show alternating bands of high and low regions on the surface of the hybrid with a uniform spacing of 18 nm.[6] These features, along with other remarkable properties of poly GT-SWCN hybrids, led Zheng et al. to propose that poly GT wraps helically about SWCN as a

* Corresponding author. E-mail: cjohnson@physics.upenn.edu.
[†] Department of Physics and Astronomy.
[‡] Department of Chemistry.

10.1021/nl071909j CCC: $40.75
Published on Web 12/11/2007

hydrogen-bonded dimer with a pitch commensurate with this 18 nm spacing.[6] Later measurements of the circular dichroism of this material also suggest helical wrapping.[11] However, AFM measurements on DNA−CN formed without sonication reveal that adsorbed ssDNA forms a thicker, presumably disordered, layer on SWCNs that is featureless in AFM.[4]

While AFM provides useful structural information on DNA−CN, its resolution is limited to several nanometers. Computer simulations, on the other hand, are well suited for gaining detailed information on nanoscale systems, such as DNA−CN, with atomic-scale resolution. Classical potentials have been employed to locate low energy conformations of ssDNA adsorbed onto SWCN.[5,10] These calculations showed that energetically favorable configurations result when ssDNA wraps helically[5] about SWCN with its bases stacked to the SWCN surface.[5,10] Ab initio computations have also been performed on single nucleotides adsorbed to SWCN to study the electronic structure of the composite system.[10]

Molecular dynamics (MD) is a computational technique that possesses several advantages over the previous methods, especially in simulations of biophysical systems.[12] MD enables investigations of dynamics and interactions during self-assembly of biomolecular complexes, as well as their structural stability. Additionally, MD simulations can include the effects of important experimental conditions such as temperature, pressure, and the aqueous environment, which were omitted in the computational work cited above. Thus, to deepen our understanding of this hybrid nanostructure, we have conducted a series of atomistic MD simulations of DNA−CNs under fully hydrated conditions.

To determine the general features of DNA−CN self-assembly, we simulated the adsorption of a 14-base random sequence ($Rand_{14}$) to an infinite SWCN in aqueous solution in accordance with typical experimental conditions.[4−9,11] We find that ssDNA undergoes significant conformational changes upon contacting SWCN, which enables the spontaneous assembly of DNA−CN mediated by the attractive $\pi-\pi$ stacking interaction between ssDNA bases and the SWCN sidewall. We have also investigated the stability of the poly GT dimer conformation proposed by Zheng et al.[6] and we find that poly GT oligonucleotides prefer to adsorb to SWCN separately and not as a dimer. Moreover, we find that the 18 nm pitch helical wrapping is structurally unstable, and a helical configuration with a more compact pitch is strongly favored. The mechanism responsible for helical wrapping is credited to electrostatic and torsional interactions within the sugar−phosphate backbone that cause ssDNA to wrap helically about SWCN from the 3′ end to the 5′ end.

Computational Methods. MD simulations were performed at constant pressure[13] (1 atm) and temperature[14] (300 K unless otherwise stated) with the GROMACS[15] MD package using a 1.5 fs time step. Electrostatic interactions were calculated with the particle mesh Ewald method,[16] and three-dimensional periodic boundary conditions were applied. To simulate an infinite SWCN, a segment with a length commensurate with the L_z box dimension was aligned along the *z*-axis with the terminal carbon atoms sharing a chemical bond. Na^+ counterions were included to exactly neutralize the negatively charged ssDNA backbone. The AMBER99 force field[17] was used to model ssDNA. On the basis of previous work,[18,19] the SWCN atoms were modeled as uncharged Lennard-Jones particles using sp^2 carbon parameters from the AMBER99 force field. The positions of all SWCN atoms were constrained with a harmonic potential. The $\pi-\pi$ stacking interaction plays a critical role in the self-assembly of DNA−CN (see below). In the AMBER99 force field, stacking interactions among aromatic species are parametrized within the van der Waals parameters of each atom type. Specific electrostatic interactions among π electrons are thus included in an average way. For further details on modeling $\pi-\pi$ stacking interactions, see ref 22. All simulations were performed with explicit solvent using the TIP3P water model.[20] However, the interior of SWCN remained hollow and devoid of water molecules in all cases, which is reasonable for pristine, unoxidized SWCNs in aqueous solution. The simulations were initialized with ssDNA in a variety of configurations as described below. In all cases, equilibrium was considered to be reached when the average root-mean-square deviation of ssDNA with respect to its starting structure no longer varied with time. Analysis and visualization of MD trajectories were performed with VMD.[21] Additional computational details are provided in the Supporting Information.

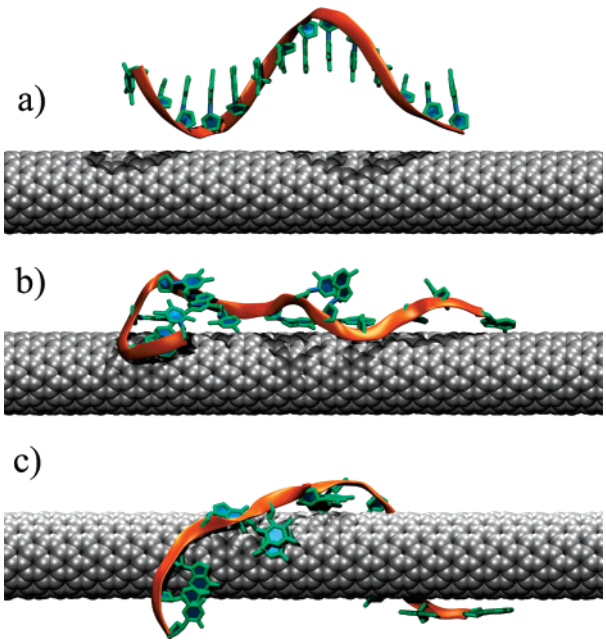

Figure 1. Self-assembly of a DNA−carbon nanotube hybrid in aqueous solution. The water molecules and Na^+ counterions have been removed for visualization purposes. (a) Initial configuration. (b) Configuration after 5.5 ns. (c) Final configuration after 21 ns.

Results and Discussion. *Self-Assembly of DNA−Carbon Nanotube Hybrids.* To obtain a microscopic picture of DNA−CN self-assembly, a simulation was performed on a random 14-base (ATCGATACGTGACT) oligonucleotide initially separated from a (11,0) SWCN by about 1.5 nm (Figure 1a). ssDNA was initialized in a helical-stacked conformation, which is a reasonable structure for short oligonucleotides in aqueous solution.[1] The system was then allowed to equilibrate over the course of MD at a constant

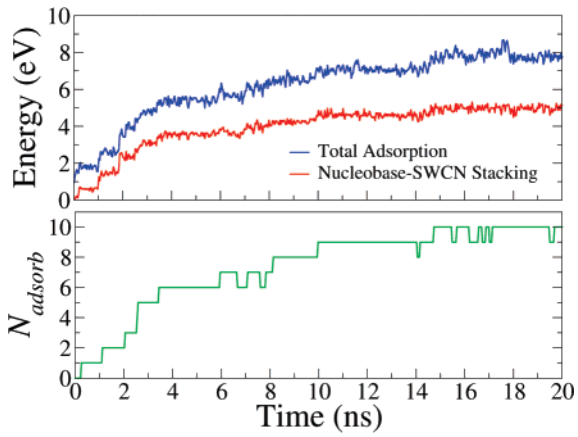

Figure 2. Total ssDNA−SWCN adsorption energy (blue) and nucelobase−SWCN stacking energy (red) and number of adsorbed nucleobases (green) as functions of time.

temperature of 330 K for 21 ns. The slightly elevated temperature was employed in this particular simulation to effectively accelerate the adsorption kinetics so that the entire process would occur within typical timescales that are accessible with MD (∼10 ns). By examining the results of approximately 20 additional simulations conducted at 300 K and involving 5 different oligonucleotides, we have verified that this temperature does not affect the mechanics involved in DNA−CN self-assembly. Thus, the results of this simulation are relevant at room temperature as well.

Within the first 500 ps, several ssDNA segments make contact to SWCN. These segments undergo a conformational change where nucleobases rotate by 90° relative to the sugar−phosphate backbone, thus becoming unstacked from their neighbors. This enables individual nucleobases to adsorb (stack) to the SWCN surface at a distance similar to that found for neighboring planes in graphite (∼0.34 nm). These nucleobases are held tightly against the SWCN sidewall and anchor ssDNA in the radial direction. However, the oligonucleotide freely diffuses along the SWCN axial and circumferential directions. Within 5.5 ns, the entire ssDNA backbone is drawn close to SWCN, which permits additional nucleobases to bind to the sidewall (Figure 1b and Figure 2). Over the next 16 ns, many of the remaining, unbound nucleobases adsorb and, even more remarkably, ssDNA spontaneously wraps around SWCN into a left-handed helix (Figure 1c).

The self-assembly of DNA−CN is driven by a strong van der Waals attraction between the faces of the nucleobases and the SWCN sidewall, that is, the $\pi-\pi$ stacking interaction.[22] The total stacking energy, which we calculate as the absolute value of the total van der Waals energy between nucleobases and SWCN, steadily increases throughout the simulation (Figure 2). This interaction is the main stabilizing force within the hybrid: it comprises 66% of the total adsorption energy of the system, even though only 43% of ssDNA atoms reside in nucleobases. Because all four nucleobases can bind via $\pi-\pi$ stacking, ssDNA of any sequence should readily form DNA−CNs. We have verified this by obtaining similar results with another random sequence as well as homopolymers (each 21 nucleotides in length) poly A, poly C, poly G, and poly T.

Although each of the four nucleobases experiences an attractive $\pi-\pi$ stacking interaction, their stacking energies vary. The purines adenine and guanine, which contain two aromatic rings, have binding energies to the (11,0) SWCN of 0.60 and 0.65 eV, respectively. The binding energies of the pyrimidines cytosine and thymine, which contain a single aromatic ring, are smaller at 0.48 and 0.55 eV, respectively. This is consistent with the expectation that the $\pi-\pi$ stacking energy should increase with increasing surface area of the faces of the interactants.[22] The binding energies thus exhibit the trend G > A > T > C, in agreement with measurements of the adsorption isotherms of nucleobases on graphite[23] and ab initio calculations of nucleobases on graphene.[24]

Perhaps the most striking result in this simulation is that ssDNA spontaneously wraps into a compact left-handed helix about SWCN circumference. In other trials with different initial configurations of the system, we observed formation of right-handed helices, achiral "loops" and disordered, kinked structures. ssDNA is a flexible polymer with many degrees of freedom and a rugged potential energy landscape containing many local minima. Thus, MD simulations of only a few tens of nanoseconds are insufficient to obtain accurate statistical information about the equilibrium distribution of these conformations at low temperatures ($T \sim 300$ K). We are conducting an analysis of the entire ensemble of low-energy ssDNA conformations about SWCN obtained using the replica exchange MD method whose results will be the subject of a future publication.

Structural Stability of Poly GT Conformations. Motivated by AFM work and the observed effectiveness of poly GT sequences in ssDNA-mediated SWCN sorting, Zheng et al. proposed that poly GT oligonucleotides form homodimeric structures held together by an exotic, non-Watson−Crick hydrogen bond network and wrap in a helical fashion about SWCNs with an 18 nm regular pitch.[6] Their proposed base pairing arrangement is shown in Figure 3a. We performed a series of simulations to examine the stability of this structure and others related to it.

First, we investigated the structural stability of this poly GT dimer. Two $(GT)_2$ oligonucleotides were constructed in linear conformations and placed adjacent to each other on a (11,0) SWCN. To facilitate dimerization, the ssDNA backbones were placed antiparallel and their bases oriented to mimic the proposed hydrogen bond pattern (Figure 3b). However, we found that this arrangement induces high stress within the ssDNA sugar residues and glycosidic bonds. Performing energy optimization on this structure alleviated this stress, but significantly altered the geometry and led to a configuration that was incompatible with the original base pairing scheme (Figure 3c). We therefore conclude that the proposed hydrogen bond pattern is energetically unfavorable and structurally unstable.

Nevertheless, the optimized structure retains some of its original hydrogen bonds (Figure 3c). To explore the possibility that these remaining bonds could stabilize a dimer, we performed a 5 ns simulation starting from this energy

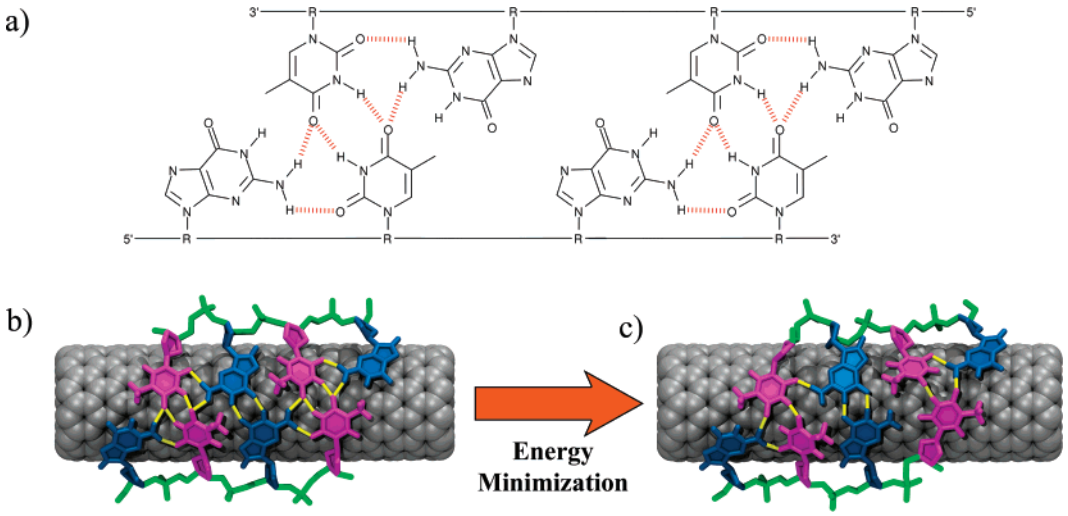

Figure 3. (a) poly GT dimer configuration proposed by Zheng et al. (b) Initial $(GT)_2$ dimer following the proposed base pair scheme. Guanine and thymine are shown in blue and magenta, respectively. Hydrogen bonds are shown in yellow. (c) $(GT)_2$ dimer after energy minimization. Several of the hydrogen bonds have been broken.

minimized configuration. The simulation results in the two strands gently separating and diffusing away from one another; no stable dimer is formed. Apparently, any attraction between the oligonucleotides is nonspecific and insufficient to survive thermal fluctuations at 300 K. It is reasonable to imagine that longer oligonucleotides containing many more inter-ssDNA hydrogen bonds would be more prone to dimerize than the short $(GT)_2$ sequences used here. However, we carried out the identical simulation using $(GT)_{20}$, a sequence ten times longer than the previous one, and obtained qualitatively similar results. The initial $(GT)_{20}$ dimer contained a total of 73 interstrand hydrogen bonds. However, after 5 ns of MD only 12 remained. These residual hydrogen bonds occurred between random bases, were not arranged in any specific fashion, and did not impose any overall structure on the adsorbed oligonucleotides.

We also considered dimer structures based on "wobble base pairing", which is known to initiate formation of double helices of poly GT sequences at low temperature.[25,26] However, this scheme is also highly unlikely to occur among adsorbed ssDNA for the following reason. In wobble base pairs, one hydrogen bond exists between atoms O6 of guanine and N3 of thymine and another between atoms N1 of guanine and O2 of thymine (Figure 4a). However, when thymine is adsorbed to SWCN, the O2 and N3 atoms are oriented toward the interior of the oligonucleotide, which restricts their ability to hydrogen bond to an opposing guanine (Figure 4b).

While this is not an exhaustive search of all possible base pairing schemes, the preceding results are evidence against the formation of stable poly GT dimers adsorbed to SWCNs. This conclusion is further corroborated by established facts about double-stranded DNA (dsDNA). In dsDNA, base pairs reside in a planar geometry that maximizes the strength of the interstrand hydrogen bonds.[1] However, the adsorbed poly GT nucleotides reside on the curved SWCN surface and are unable to form planar base pairs. This geometry significantly

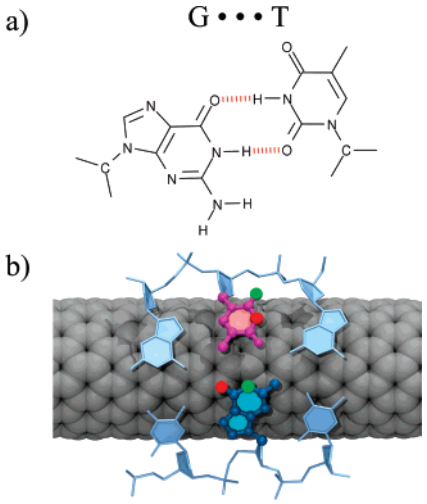

Figure 4. (a) G−T wobble base pair. (b) Two poly GT strands adsorbed to SWCN. Guanine and thymine are shown in blue and magenta, respectively. Atom pairs that would normally share hydrogen bonds in a wobble base pair are colored red and green, respectively. The geometry assumed by adsorbed nucleobases makes them incompatible with wobble base pairing.

reduces the cohesive strength of interstrand hydrogen bonds. Additionally, in dsDNA, adjacent bases are stacked on top of one another in a spiral staircase fashion.[1] Because of this stacked geometry, bases are freely able to hydrogen bond to their counterparts without steric hindrance. These stacking interactions also provide rigidity in dsDNA and are as important as base pair interactions in stabilizing the double helix.[1] However, in the adsorbed state, adjacent poly GT bases lie roughly in the same plane and must compete for space on the SWCN surface. Thus, adsorbed bases are subjected to steric restrictions that impede their ability to form base pairs. Also, because of the lack of intrastrand stacking interactions, adsorbed poly GT adopts a more disordered structure compared to dsDNA. Consequently, interstrand interactions among the adsorbed oligonucleotides tend to be more random and nonspecific.

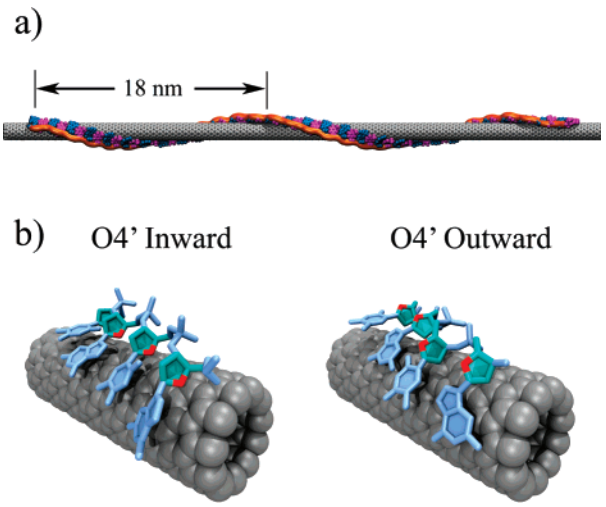

Figure 5. (a) $(GT)_{30}$ on a (11,0) SWCN with regular 18 nm pitch. (b) Different sugar−phosphate backbone orientations with respect to SWCN. O4′ (red) points either radially inward or outward from SWCN.

Because we find that dimer formation is improbable, we performed several simulations of a single adsorbed poly GT oligonucleotide to determine the stability of helically wrapped poly GT. We constructed a (11, 0) SWCN initially wrapped with a 60 base long poly GT ($(GT)_{30}$) sequence adopting an 18 nm pitch helix (Figure 5a). This oligonucleotide is identical to that used by Zheng et al. in their original AFM experiments. Because of the chiral ssDNA backbone, we identified four distinct conformations consistent with helical wrapping. These structures differ in helical handedness (left or right) or orientation of the sugar−phosphate backbone with respect to SWCN. For clarity, the backbone orientation is defined by the position of the O4′ atom of the sugar group, which can point radially inward or outward from SWCN (Figure 5b). Thus, the four initial structures are LH-inward, LH-outward, RH-inward, and RH-outward, where LH and RH stand for left-handed and right-handed, respectively. In each case, ssDNA was initialized with 26 bases per helical turn. This value was determined to minimize both steric repulsion between adjacent nucleobases and bond stretching of the backbone under the constraint of an 18 nm pitch. Each structure was relaxed over the course of 80−100 ns in aqueous solution.

In each system, $(GT)_{30}$ retains a helical wrapping about SWCN but undergoes an overall reduction in pitch. The final pitch values for the four systems range from 2 nm for LH-outward to 8 nm for RH-inward. The decrease in pitch is accompanied by an increase in the number of helical turns about SWCN circumference. These results indicate that helical wrapping is a viable ssDNA structure about SWCN. However, pitch values over about 10 nm are unfavorable.

Strikingly, the inward and outward ssDNA conformations are energetically distinguishable; the inward structure has the lower potential energy by 0.11 eV/nucleobase. This energetic difference is largely due to the ssDNA−water and ssDNA−SWCN interactions. Compared to the outward conformation, adjacent nucleobases residing in the inward conformation tend to be more spatially separated and more heavily solvated by water. As a result, each thymine has approximately 0.67 more hydrogen bonds with water for the inward conformation. Additionally, the inward ssDNA backbone is about 0.8 Å closer to SWCN, which results in a more favorable ssDNA−SWCN van der Waals interaction.

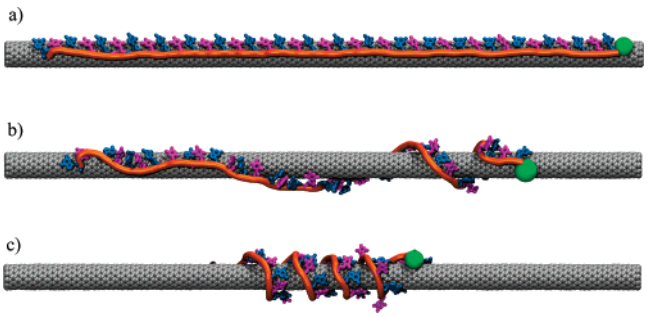

Figure 6. Simulation of S_1 displaying right-handed helical wrapping of $(GT)_{20}$ about SWCN. (a) Initial configuration. (b) Configuration after 2.2 ns. (c) Configuration after 7 ns. The green sphere marks the ssDNA 3′ end. Similar results occur for S_2, but with left-handed helical wrapping.

Mechanism for Helical Wrapping. To investigate the mechanism responsible for ssDNA helical wrapping, we carried out simulations of two systems, S_1 and S_2, where a $(GT)_{20}$ oligonucleotide initially adopts a linear, ahelical conformation on top of a (11,0) SWCN (Figure 6a). In each system, ssDNA was initialized in the inward configuration but with a different set (α, β, γ, δ, ϵ, ζ) of backbone torsion angles. The initial average torsional angles were (260, 162, 59, 140, 159, and 135°) and (194, 116, 62, 104, 143, and 216°) for S_1 and S_2, respectively. Each system was allowed to relax in aqueous solution for 7 ns.

Remarkably, the linear oligonucleotide in S_1 and S_2 spontaneously winds around the SWCN into a right- and left-handed helix, respectively. In both systems, helical wrapping does not occur uniformly over the entire length of the oligonucleotide. Instead, the ssDNA 5′ end remains essentially stationary (apart from thermal motion) while the 3′ end rapidly encircles the SWCN circumference (Figure 6b). As a result, additional helical turns are generated at the 3′ end, which then propagate toward the 5′ end. The winding continues until ssDNA forms a compact helix about SWCN (Figure 6c).

Analysis of structural and energetic changes that occur in the two systems reveals that electrostatic interactions within the ssDNA backbone are responsible for wrapping the initially linear oligonucleotide into a helical structure. As the helix forms, the average distance between adjacent phosphates (d_{P-P}) steadily increases, thereby relieving electrostatic repulsion (E_{P-P}) within the backbone (Figure 7). These structural changes proceed via a rearrangement of the backbone torsional angles (Figure 7). It is apparent that the differing initial sets of torsional angles in S_1 and S_2 enable ssDNA to evolve along two drastically different pathways that ultimately lead to a right- and left-handed structure, respectively. The importance of backbone torsion in helix formation is most likely why the wrapping occurs asymmetrically with turns being generated at the 3′ end. The chiral sugar−phosphate backbone results in chiral forces along the

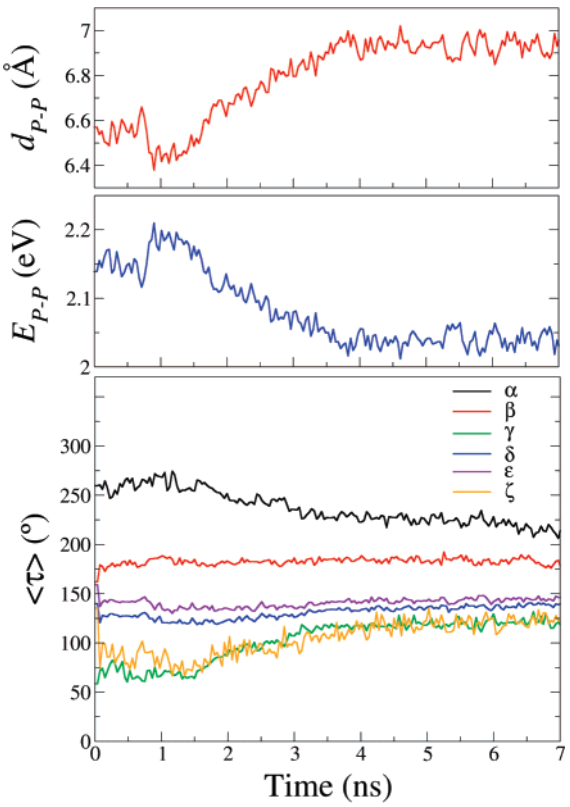

Figure 7. Structural and energetic changes for S_1. The average distance (d_{P-P}) between adjacent phosphorus atoms (top) increases as the helix forms, thereby reducing the electrostatic repulsion (E_{P-P}) between them (middle). These changes proceed via a rearrangement of the average torsional angles ($<\tau>$) in the ssDNA backbone (bottom). Qualitatively similar data (not shown) occurs for S_2.

oligonucleotide, which may facilitate deformations along preferred directions.

It should be pointed out that the preceding observations arise from the artificial initial condition of linear ssDNA, and that it is possible that other nonhelical conformations may result from a more random initial configuration. However, these results provide several interesting insights about the mechanics of oligonucleotides adsorbed to SWCN. First, the sugar−phosphate backbone contains intrinsic curvature and prefers a helical wrapping to a linear structure. Second, while $\pi-\pi$ stacking is the main driving force for DNA−CN self-assembly, the backbone dictates the overall ssDNA conformation. Because the sugar−phosphate backbone is not specific to base sequence, general ssDNA sequences are thus expected to wrap SWCN in a similar manner to that observed here. We have verified this by obtaining similar results with a random 40-base long sequence. There is also reason to believe that the 3′ to 5′ wrapping may be a general feature of DNA−CN as it has been observed in other systems with differing initial conditions. For example, in the previously described simulations involving the relaxation of the $(GT)_{30}$ 18 nm pitch helices, the overall reduction of pitch and increase in the number of helical turns also proceeded via a 3′ to 5′ wrapping.

It is widely appreciated that electrostatics play a vital role in DNA deformation[1,27] and in the polymorphism of the double helix.[1] For example, the form[1] and mechanical properties[28] of the double helix are extremely sensitive to the salt concentration of the solvent. Cations alter the dielectric properties of the solvent and screen electrostatic repulsion between phosphates. We have observed salt concentration dependent effects in our simulations as well. Adding 0.5 M NaCl to S_1 and S_2 effectively neutralizes the negatively charged backbone and quenches helical wrapping.

Effect of SWCN Chirality. All simulations presented here involve a zigzag SWCN whereas, experimentally, ssDNA encounters SWCNs of widely distributed chirality. To gain insight on how SWCN chirality affects ssDNA conformation, we calculated the energy of an adsorbed guanine at various positions along the axis of a (6,6) armchair and (11,0) zigzag SWCN. The energy barriers for lateral motion of guanine across the SWCN surface of either chirality are less than k_BT. Specifically, these barriers are 0.4 k_BT and 0.6 k_BT for the armchair and zigzag SWCN, respectively. This suggests that at room temperature, the SWCN potential presents only small barriers for lateral movement of adsorbed nucleobases, in agreement with molecular mechanics calculations of adenine on graphite.[29] Thus, the orientation of adsorbed nucleobases will be quite insensitive to SWCN chirality. The energy corrugation found in these simulations is somewhat smaller than the values of 1.2−4 k_BT obtained from ab initio calculations of single nucleobases on graphene[24,30] or SWCN.[31] However, because the driving force for the helical wrapping is due to the ssDNA backbone, it is reasonable that all sequences can conform to SWCN of general chirality in a helical manner consistent with the results reported here.

Conclusion. We have conducted a series of atomistic MD simulations that explore the self-assembly mechanisms, structure, and energetic properties of DNA−CN. We find that in aqueous solution, the presence of SWCN induces a conformational change in ssDNA that enables oligonucleotides of general sequence to adsorb via the $\pi-\pi$ stacking interaction. The stacking interaction is attractive for all four nucleobases with purines exhibiting the strongest binding. The flexibility of ssDNA enables a wide range of wrapping conformations about SWCNs including right- and left-handed helices, achiral "loops" and disordered, kinked structures. Helix formation for adsorbed oligonucleotides is found to derive from electrostatic and torsional interactions within the sugar−phosphate backbone, which results in ssDNA wrapping about SWCN from the 3′ end to the 5′ end. Because the driving forces for ssDNA adsorption and helix formation are both independent of the specific base sequence, general ssDNA sequences are thus expected to wrap SWCN in a similar manner to that observed here. However, several experiments[4,6] involving DNA−CN reveal that ssDNA base sequence plays a prominent role in the physical and chemical properties of the resulting hybrid. While we find that that sequence does not affect the coarse structure of DNA−CN, there must be higher order, sequence-dependent effects, such as solvation patterns or intra-ssDNA nucleotide−nucleotide interactions, that are important.

Within the limitations of the force fields employed here, we find that the poly GT dimer proposed by Zheng et al.

and related configurations are structurally unstable. Hybridization between multiple adsorbed poly GT oligonucleotides is unfavorable due to geometric factors. This has important ramifications for experiments using DNA−CN to detect DNA hybridization. It is possible that the traditional base pairing scheme between complimentary oligonucleotides may be hindered when one strand is adsorbed to SWCN. This is consistent with the interpretations of experiments involving DNA-functionalized SWCN FETs for detection of DNA hybridization.[9]

Adsorbed ssDNA is found to prefer a compact helical wrapping with a pitch much less than 18 nm at the low salt concentrations employed here. We find that at high salt concentration, helical wrapping could be suppressed entirely. It remains an open question whether a more elongated helical structure is preferred at intermediate salt concentrations. We note that in the AFM measurements by Zheng et al., DNA−CNs were dried in air prior to imaging thus altering the dielectric environment around the hybrids from that in aqueous solution. This may result in ssDNA conformations that differ from those found in a fully hydrated DNA−CN.

While it is commonplace to visualize DNA as a helical structure, it is important to note that the conformations found here would not result without the presence of SWCN. Upon adsorption, SWCN provides a cylindrical template for helical wrapping. The resulting ssDNA conformations in DNA−CN are drastically different than those found in double-stranded DNA or even in ssDNA in aqueous solution. Thus, as research proceeds in combining inorganic nanomaterials with biological molecules, objects that have never been in contact in nature, there is a great possibility of discovering composite materials, such as DNA−CNs, that possess brand new structural and physical properties.

Acknowledgment. We thank Dr. Katrin Spiegel for many useful discussions about the physical properties of DNA. We thank Dr. Matteo Dal Perraro and Dr. Axel Kohlmeyer for generous and insightful advice on simulations of biomolecular systems. This work was supported by NSF MRSEC Grant 0520020 and JSTO, DTRA, and the Army Research Office Grant W911NF-06-1-0462.

Supporting Information Available: Additional computational details of the simulations. This material is available free of charge via the Internet at http://pubs.acs.org.

References

(1) Saenger, W. *Principles of nucleic acid structure*; Springer-Verlag: New York, 1984.
(2) Breaker, R. R. *Nature* **2004**, *432* (7019), 838−845.
(3) Saito, R.; Dresselhaus, G.; Dresselhaus, M. S. *Physical properties of carbon nanotubes*; Imperial College Press: London, 1998.
(4) Staii, C.; Chen, M.; Gelperin, A.; Johnson, A. T. *Nano Lett.* **2005**, *5* (9), 1774−1778.
(5) Zheng, M.; Jagota, A.; Semke, E. D.; Diner, B. A.; Mclean, R. S.; Lustig, S. R.; Richardson, R. E.; Tassi, N. G. *Nat. Mater.* **2003**, *2* (5), 338−342.
(6) Zheng, M.; Jagota, A.; Strano, M. S.; Santos, A. P.; Barone, P.; Chou, S. G.; Diner, B. A.; Dresselhaus, M. S.; Mclean, R. S.; Onoa, G. B.; Samsonidze, G. G.; Semke, E. D.; Usrey, M.; Walls, D. J. *Science* **2003**, *302* (5650), 1545−1548.
(7) Jeng, E. S.; Moll, A. E.; Roy, A. C.; Gastala, J. B.; Strano, M. S. *Nano Lett.* **2006**, *6* (3), 371−375.
(8) Star, A.; Tu, E.; Niemann, J.; Gabriel, J. C. P.; Joiner, C. S.; Valcke, C. *Proc. Natl. Acad. Sci. U.S.A.* **2006**, *103* (4), 921−926.
(9) Tang, X. W.; Bansaruntip, S.; Nakayama, N.; Yenilmez, E.; Chang, Y. L.; Wang, Q. *Nano Lett.* **2006**, *6* (8), 1632−1636.
(10) Meng, S.; Maragakis, P.; Papaloukas, C.; Kaxiras, E. *Nano Lett.* **2007**, *7* (1), 45−50.
(11) Dukovic, G.; Balaz, M.; Doak, P.; Berova, N. D.; Zheng, M.; Mclean, R. S.; Brus, L. E. *J. Am. Chem. Soc.* **2006**, *128* (28), 9004−9005.
(12) Karplus, M.; McCammon, J. A. *Nat. Struct. Mol. Biol.* **2002**, *9* (9), 646−652.
(13) Parrinello, M.; Rahman, A. *J. Appl. Phys.* **1981**, *52* (12), 7182−7190.
(14) Berendsen, H. J. C.; Postma, J. P. M.; Vangunsteren, W. F.; Dinola, A.; Haak, J. R. *J. Chem. Phys.* **1984**, *81* (8), 3684−3690.
(15) Lindahl, E.; Hess, B.; van der Spoel, D. *J. Mol. Model.* **2001**, *7* (8), 306−317.
(16) Darden, T.; York, D.; Pedersen, L. *J. Chem. Phys.* **1993**, *98* (12), 10089−10092.
(17) Cornell, W. D.; Cieplak, P.; Bayly, C. I.; Gould, I. R.; Merz, K. M.; Ferguson, D. M.; Spellmeyer, D. C.; Fox, T.; Caldwell, J. W.; Kollman, P. A. *J. Am. Chem. Soc.* **1995**, *117* (19), 5179−5197.
(18) Hummer, G.; Rasaiah, J. C.; Noworyta, J. P. *Nature* **2001**, *414* (6860), 188−190.
(19) Zou, J.; Ji, B.; Feng, X. Q.; Gao, H. *Nano Lett.* **2006**, *6* (3), 430−434.
(20) Jorgensen, W. L. *J. Am. Chem. Soc.* **1981**, *103* (2), 335−340.
(21) Humphrey, W.; Dalke, A.: Schulten, K. *J. Mol. Graphics* **1996**, *14*, 33−38.
(22) Hunter, C. A.; Sanders, J. K. M. *J. Am. Chem. Soc.* **1990**, *112* (14), 5525−5534.
(23) Sowerby, S. J.; Cohn, C. A.; Heckl, W. M.; Holm, N. G. *Proc. Natl. Acad. Sci. U.S.A.* **2001**, *98* (3), 820−822.
(24) Gowtham, S.; Scheicher, R. H.; Ahuja, R.; Pandey, R.; Karna, S. P. *Phys. Rev. B* **2007**, *76*, 033401−033403.
(25) Early, T. A.; Olmsted, J.; Kearns, D. R.; Lezius, A. G. *Nucleic Acids Res.* **1978**, *5* (6), 1955−1970.
(26) Gray, D. M.; Ratliff, R. L. *Biopolymers* **1977**, *16* (6), 1331−1342.
(27) Williams, L. D. *Annu. Rev. Biophys. Biomol. Struct* **2000**, *29*, 497−521.
(28) Baumann, C. G.; Smith, S. B.; Bloomfield, V. A.; Bustamante, C. *Proc. Natl. Acad. Sci. U.S.A.* **1997**, *94* (12), 6185−6190.
(29) Edelwirth, M.; Freund, J.; Sowerby, S. J.; Heckl, W. M. *Surf. Sci.* **1998**, *417* (2−3), 201−209.
(30) Ortmann, F.; Schmidt, W. G.; Bechstedt, F. *Phys. Rev. Lett.* **2005**, *95* (18), 186101.
(31) Meng, S.; Wang, W. L.; Maragakis, P.; Kaxiras, E. *Nano Lett.* **2007**, *7* (8), 2312−2316.

NL071909J